Decentralised binary detection with non-constant SNR profile at the sensors

Gianluigi Ferrari*

Wireless Ad-hoc and Sensor Networks (WASN) Laboratory,
Information Engineering Department,
University of Parma,
Parma, Italy
E-mail: gianluigi.ferrari@unipr.it
*Corresponding author

Roberto Pagliari

Electrical and Computer Engineering Department,
Cornell University,
Ithaca, NY, USA
E-mail: rp294@cornell.edu

Marco Martalò

Wireless Ad-hoc and Sensor Networks (WASN) Laboratory,
Information Engineering Department,
University of Parma,
Parma, Italy
E-mail: martalo@tlc.unipr.it

Abstract: In this paper, we consider the problem of decentralised binary detection in sensor networks characterised by *non-constant* observation Signal-to-Noise Ratios (SNRs) at the sensors. In general, SNRs at the sensors could have a *generic* non-constant distribution. In order to analyse the performance of these decentralised detection schemes, we introduce the concept of sensor *SNR profile*, and we consider four possible profiles (linear, quadratic, cubic and hyperbolic) as representative of a large number of realistic scenarios. Furthermore, we show *how* the impact of communication noise in the links between the sensors and the Access Point (AP) depends on the sensor SNR profile (i.e. the spatial distribution of the observation noise). More precisely, different sensor SNR profiles are compared under two alternative assumptions: (i) common *maximum* sensor SNR or (ii) common *average* sensor SNR. Finally, we propose an *asymptotic* (for a large number of sensors) performance analysis, deriving a simple expression for the limiting probability of decision error. We validate our theoretical analysis with experimental results.

Keywords: decentralised detection; sensor networks; Signal-to-Noise Ratio; SNR; sensor SNR profile; noisy communication links.

Biographical notes: Gianluigi Ferrari received the 'Laurea' (a five-year program) (*summa cum laude*) and the PhD degrees in Electrical Engineering from the University of Parma, Parma, Italy, in 1998 and 2002, respectively. Since 2002 he has been a Research Professor at the Department of Information Engineering (DII), University of Parma, Italy, where he is now the Coordinator of the Wireless Ad-hoc and Sensor Networks (WASN) lab. He also visited the University of Southern California, USA, and Carnegie Mellon University, USA. His research interests include adaptive signal processing, information theory and wireless ad hoc and sensor networking. He is a corecipient of a best student paper award at the *2006 International Workshop on Wireless Ad hoc Networks* (IWWAN'06).

Roberto Pagliari received the 'Laurea' degree in Electrical Engineering from the University of Parma, Italy, in 2005. He is currently working towards the PhD degree at Cornell University, Ithaca, NY, USA. His research is focused on distributed protocols for sensor networks.

Marco Martalò received the 'Laurea' degree in Telecommunication Engineering from the University of Parma, Parma, Italy, in 2005. Since 2006, he is a PhD student in the WASN

Lab, DII, University of Parma. Between 2007 and 2008 he was a Visiting Scholar at Ecole Polytechnique Féderale de Lausanne (EPFL), Switzerland. His research interests include digital communication systems design, information theory and wireless sensor networking. He is a corecipient of a best student paper award at IWWAN'06.

1   Introduction

Recent years have witnessed an increasing interest for the use of distributed detection techniques in sensor networks, especially for civilian applications, e.g. environmental monitoring. The application of distributed detection techniques in the military field has, on the other hand, a long history. In all cases, the goal of a sensor network with distributed detection is to identify the status of a phenomenon of interest through a collaborative action of the sensors. In several situations, however, the sensors might *observe* the same phenomenon with *varying quality*. In other words, while some sensors might have direct access to the phenomenon (e.g. they are close to a monitored source of heat), other sensors might not (e.g. there is an obstruction between them and the target source of heat). Therefore, a relevant problem, with practical implications, consists in evaluating the performance of distributed detection schemes with non-constant observation quality at the sensors.

Distributed detection has been an active research field for a long time. In particular, several approaches have been proposed to study this problem (Reibman and Nolte, 1981; Hoballah and Varshney, 1989). The increasing interest, over the last decade, for sensor networks, has spurred a further research activity burst on distributed detection techniques in this context (Blum et al., 1997; Viswanathan and Varshney, 1997; Chong and Kumar, 2003). The impact of communication constraints, e.g. limited bandwidth and presence of noise, is considered in Gini et al. (1998), where a randomisation paradigm for decentralised detection is proposed to overcome the communication bottle-neck. In Chen et al. (2004), the authors consider the problem of decentralised detection in *wireless* sensor networks where communication links are affected by fading. In the latter scenario, the optimal distributed detection strategy is first derived on the basis of the integration of the communication and fusion phases, and then suboptimal (requiring a limited a priori knowledge of the channel state) strategies are developed. This approach is further extended in Chen and Willett (2005), where the authors optimise the local decision strategy in sensor networks with fading, and in Jiang and Chen (2005), where the authors propose a decentralised detection strategy based on censoring sensors, which transmit only when their local likelihood ratios are sufficiently large.

In Ferrari and Pagliari (2006), a communication-theoretic-oriented framework for performance analysis of sensor networks with noisy communication links is proposed. While in Ferrari and Pagliari (2006) a *common* value for the Signal-to-Noise Ratio (SNR) at the sensors is considered, in this paper, we assume that the sensors observe a common binary phenomenon with *different* SNRs. The sequence of sensor SNRs is referred to as *sensor SNR profile*. Provided that the original sensor SNRs are properly rearranged, without loss of generality one can consider only monotonically *non-increasing* profiles.

Since it is reasonable to assume that linear, quadratic, cubic and hyperbolic sensor SNR profiles can be representative of a large number of realistic situations, we use these profiles to investigate the impact of non-constant sensor SNRs on the performance of the considered decentralised detection schemes. The comparison between the performance of networks with different sensor SNR profiles is carried out in scenarios where either the maximum or the average sensor SNR is kept constant. Our results show that, for a given sensor SNR profile, selection of a proper subset of the sensors leads to a minimisation of the probability of decision error at the access point (AP). More precisely, for *very steep* sensor SNR profiles (i.e. very irregular sensor SNR distribution without rearrangement in a non-increasing order), it turns out that the best performance is obtained by selecting only the sensors with the highest SNRs (asymptotically, only *the* sensor with highest SNR). We also investigate the network performance in a theoretical scenario where sensors do not take binary decisions on the observed phenomenon, but transmit the conditional Probability Density Functions (PDFs) of their observable. Since the focus of this paper is on the impact of varying *observation quality* at the sensors, we consider a simple model, given by Binary Symmetric Channel (BSC), for a noisy *communication* link and we assume that the noise intensity (given by the cross-over probability of BSC) is the same for all links. Our approach could be extended considering also varying quality of the communication links – for instance, this would correspond to different cross-over probabilities according to the considered BSC model. Based on the use of the De Moivre–Laplace approximation (Papoulis, 1991), we apply our framework to analyse the network performance in an asymptotic (for very large values of the number of sensors) regime. Finally, an experimental set-up is considered to determine a realistic sensor SNR profile. The most suited profile for the considered experimental scenarios turns out to be *linear*.

This paper is structured as follows. In Section 2, we provide the reader with important mathematical preliminaries on binary decentralised detection in sensor networks. In Section 3, the probability of decision error is derived in different scenarios: (i) with ideal communication links (Subsection 3.1), (ii) with noisy communication links (Subsection 3.2) and (iii) with no quantisation at the sensors (Subsection 3.3). In Section 4, we characterise the sensor SNR profile, whereas in Section 5 the obtained performance results are discussed. In Section 6, an asymptotic (for a large number of sensors) performance analysis is presented. In Section 7, two simple experiments are proposed to determine a realistic sensor SNR profile. Finally, conclusions are drawn in Section 8.

2 Preliminaries

The focus of this paper is on a classical sensor network scenario where all sensors observe a *common* phenomenon and are connected to a single AP (Viswanathan and Varshney, 1997). In particular, we consider *binary* decentralised detection, in the sense that the observed phenomenon can assume two possible values. We denote these two hypotheses as H_0 and H_1, respectively. The observation at the *i*th sensor, at a given epoch,[1] can be expressed as

$$r_i = H \cdot s_i + n_i, \quad i = 1, 2, \ldots, N$$

where s_i is the intensity of the phenomenon observed at the *i*th sensor and n_i is the observation noise at the same sensor. Assuming that the noise samples $\{n_i\}$ are independent and have the Gaussian distributions $\left\{ \mathcal{N}\left(0, \sigma_i^2\right) \right\}$, SNR at the *i*th sensor can be defined as

$$\text{SNR}_{\text{sensor}}^{(i)} \triangleq \frac{\left[\mathbf{E}\left\{ r_i | H_1 \right\} - \mathbf{E}\left\{ r_i | H_0 \right\} \right]^2}{\sigma_i^2} = \frac{s_i^2}{\sigma_i^2}.$$

In order to make a decision, the *i*th sensor compares the observation r_i with a threshold value τ_i and computes a binary decision $u_i \triangleq U(r_i - \tau_i)$, where $U(\cdot)$ is the unit step function. Once all sensors have made their local decisions $\{u_i\}$, the AP receives[2] an array of N binary values, and makes a final decision u_0 according to a proper fusion rule $u_0 = \Gamma\left(u_1^{\text{rec}}, \ldots, u_N^{\text{rec}}\right)$. In a scenario with the same SNR at all sensors $\left(\text{SNR}_{\text{sensor}}^{(i)} = \text{constant}\right)$, the considered fusion rule is the following *majority-like* fusion rule (Reibman and Nolte, 1988):

$$\Gamma\left(u_1^{\text{rec}}, \ldots, u_N^{\text{rec}}\right) = \begin{cases} 1 & \text{if} \quad \sum_{i=1}^N u_i^{\text{rec}} \geq k \\ 0 & \text{if} \quad \sum_{i=1}^N u_i^{\text{rec}} < k \end{cases}. \tag{1}$$

While the described approach is based on the assumption that each sensor makes a hard binary decision, i.e. binary quantisation at the sensors is considered, it can be extended to a theoretical scenario where *no quantisation* is carried out at the sensors. In other words, each sensor transmits to AP its *local likelihood value* – this extension is the subject of Subsection 3.3.

Consider now a generic scenario with different SNRs at the sensors. In this case, a decision based on the *majority-like* fusion rule (equation 1) might not be the best choice. In fact, if a sensor is very noisy (i.e. its observation SNR is very small), its decision should be taken into account with a low level of reliability in the fusion process at AP. Therefore, it would be reasonable to assign each sensor a weight proportional to its own SNR – this approach is similar to that proposed in Chen et al. (2004), where the weights are assigned according to the link qualities. AP could then make a final decision taking into account the weights assigned to the sensors. Note that the improvement, in terms of probability of decision error, comes at the price of non-optimal network energy efficiency, since all

sensors, even those with low SNR, have to send their decisions to the AP and waste the same amount of energy.

In the following, we consider a system where the AP takes into account the N local sensor decisions with the same weight, i.e. without considering their SNRs, and adopts a majority-like decision rule (as in equation 1). In order to take into consideration the sensor SNR profile, the threshold for local decision at each sensor is properly optimised, as explained in detail in Subsection 3.1.2.

3 Probability of decision error

The probability of decision error can be generally written as

$$P_e \triangleq P\left(u_0 \neq H\right) = P\left(u_0 = H_1 | H = H_0\right) P(H_0) \\ + P\left(u_0 = H_0 | H = H_1\right) P(H_1) \tag{2}$$

where H is the true hypothesis.[3] We now derive analytical expressions for equation (2), distinguishing between a scenario with *ideal* communication links and a scenario with *noisy* communication links. We also derive an analytical expression for equation (2) when no quantisation is carried out at the sensors, i.e. when sensors transmit their local likelihood values.

3.1 Ideal communication links

3.1.1 Probability of decision error

Consider the first conditional probability at the right-hand side of equation (2) and recall the threshold value k in the majority-like decision rule (equation 1). There is an error, i.e. $u_0 = H_1$ given that $H = H_0$, if $i \geq k$ sensors decide for H_1 when H_0 has happened. In this case, there can be $\binom{N}{i}$ combinations of sensors deciding for H_1. We denote as $\Omega_i(j)$ the *j*th possible combination $\left(j = 1, \ldots, \binom{N}{i}\right)$ in a scenario where i sensors are in error.[4] Therefore, the conditional probability of interest can be expressed as follows:

$$P\left(u_0 = H_1 | H_0\right) = \sum_{i=k}^N \sum_{j=1}^{\binom{N}{i}} \left\{ \prod_{l=1}^i P\left(u_l^{(\Omega_i(j))} = H_1 | H_0\right) \\ \cdot \prod_{m=i+1}^N P\left(u_m^{(\Omega_i(j))} = H_0 | H_0\right) \right\} \tag{3}$$

where $P\left(u_l^{(\Omega_i(j))} = H_1 | H_0\right)$ is the probability that at the *l*th sensor, in the $\Omega_i(j)$th combination (out of the $\binom{N}{i}$ possible ones), a wrong decision is made when H_0 has happened.

Similarly, the second conditional probability at the right-hand side of equation (2) can be expressed as

$$P\left(u_0 = H_0 | H_1\right) = \sum_{i=0}^{k-1} \sum_{j=1}^{\binom{N}{i}} \left\{ \prod_{l=1}^i P\left(u_l^{(\Omega(j))} = H_1 | H_1\right) \\ \cdot \prod_{m=i+1}^N P\left(u_m^{(\Omega(j))} = H_0 | H_1\right) \right\} \tag{4}$$

where $P\left(u_l^{(\Omega_i(j))} = H_1 \middle| H_1\right)$ is the probability that at the lth sensor, in the $\Omega_i(j)$th combination, a correct decision is made when H_1 has happened.

3.1.2 Decision threshold selection at the sensors

In the literature, it is shown that using the same threshold at all sensors is an asymptotically optimal solution *if and only if* SNR at the sensors is constant (Tsitsiklis, 1988). In the currently considered scenario (with different SNRs at the sensors), it is not reasonable to use the same threshold at all sensors. Therefore, one needs to choose another criterion for local decisions at the sensors.

In this paper, we consider a *locally optimal* decision scheme.[5] In other words, each sensor makes a binary decision which minimises, for the corresponding SNR, its probability of (local) error − this corresponds to a *Person-By-Person Optimisation* (PBPO) approach to decentralised detection (Alhakeem and Varshney, 1995). The optimal value for the threshold τ_i is such that

$$p\left(\tau_i \middle| H_1\right)P(H_1) = p\left(\tau_i \middle| H_0\right)P(H_0) \tag{5}$$

where $p\left(\tau_i \middle| H_1\right) \propto e^{-(\tau_i - s_i)^2/2\sigma_i^2}$ and $p\left(\tau_i \middle| H_0\right) \propto e^{-(\tau_i^2/2\sigma_i^2)}$. From equation (5), one readily obtains that the optimal local threshold at the ith sensor is

$$\tau_i = \frac{s_i}{2} + \frac{\sigma_i^2}{s_i}\ln\frac{P(H_0)}{1 - P(H_0)}. \tag{6}$$

In the presence of ideal communication links from the sensors to AP, a generic term in equations (3) and (4) can be written as

$$\begin{aligned} P\left(u_l = H_1 \middle| H\right) &= P\left(r_l > \tau_l \middle| H\right) \\ &= P\left(s_l \cdot H + n_l > \tau_l\right) \\ &= 1 - \Phi\left(\frac{\tau_l - s_l \cdot H}{\sigma_l}\right) \end{aligned} \tag{7}$$

where $\Phi(x) \triangleq 1/\sqrt{2\pi}\int_{-\infty}^{x} e^{-(y^2/2)}\mathrm{d}y$. In general, the computation of the probability of decision error, based on the evaluation of equations (3) and (4), depends on (i) the chosen value for k, (ii) the sequence of the detected phenomenon amplitudes $\{s_i\}$ at the sensors, (iii) the sequence of noise variances $\{\sigma_i\}$ and (iv) the sequence of thresholds $\{\tau_i\}$. Using equation (6) in equation (7), one obtains

$$\begin{aligned} \Phi\left(\frac{\tau_l - s_l \cdot H}{\sigma_l}\right) = \Phi\Bigg(&\frac{1}{2}\sqrt{\mathrm{SNR}_{\mathrm{sensor}}^{(l)}} \\ &+ \frac{1}{\sqrt{\mathrm{SNR}_{\mathrm{sensor}}^{(l)}}}\ln\frac{P(H_0)}{1 - P(H_0)} - \sqrt{\mathrm{SNR}_{\mathrm{sensor}}^{(l)}}\,H\Bigg). \end{aligned}$$

As expected, the probability of decision error does not depend on the sequences $\{s_i\}$ and $\{\sigma_i\}$ separately but, rather, only on the sequence of ratios $\{s_i/\sigma_i\}$, i.e. on the sequence of sensor SNRs. In other words, the probability of decision error depends on the sensor *SNR profile* $\left\{\mathrm{SNR}_{\mathrm{sensor}}^{(i)}\right\}$. Therefore, evaluating the system performance of the sensor network as a function of the sensor SNR profile is a meaningful problem.

3.2 Noisy communication links

In a realistic wireless communication scenario, communication links between the sensors and AP may be *noisy*. In Ferrari and Pagliari (2006), it is shown how to extend the previous approach for the evaluation of the probability of decision error to a scenario where some of the links from the sensors to AP are noisy. As a general model for a noisy link, we consider a BSC.

Let us denote by p the cross-over probability of BSCs (the same for all noisy communication links). In this case, the decision made at the lth sensor, i.e. u_l, might be 'flipped', with probability p, by the communication link. In particular, the component conditional probabilities in equation (2) depend on p. For instance, the conditional probability (3) has to be modified by replacing the decisions made locally by the sensors with the corresponding *received* decisions:

$$\begin{aligned} P\left(u_0 = H_1 \middle| H_0\right) = \sum_{i=k}^{N}\sum_{j=1}^{\binom{N}{i}}\Bigg\{&\prod_{l=1}^{i} P\left(u_l^{(\Omega_i(j))-\mathrm{rec}} = H_1 \middle| H_0\right) \\ &\cdot \prod_{m=i+1}^{N} P\left(u_m^{(\Omega_i(j))-\mathrm{rec}} = H_0 \middle| H_0\right)\Bigg\} \end{aligned} \tag{8}$$

where $u_l^{(\Omega_i(j))-\mathrm{rec}}$ and $u_m^{(\Omega_i(j))-\mathrm{rec}}$ are the received versions of the local decisions $u_l^{(\Omega_i(j))}$ and $u_m^{(\Omega_i(j))}$, respectively. The conditional probability (4) has to be modified similarly. A generic term in equation (8) can then be expressed as follows:

$$P\left(u_l^{\mathrm{rec}} = H_1 \middle| H_0\right) = (1-p)\left[1 - \Phi\left(\frac{\tau_l}{\sigma_l}\right)\right] + p\Phi\left(\frac{\tau_l}{\sigma_l}\right). \tag{9}$$

Since we are considering locally optimal selection of the decision thresholds at the sensors, there is no difference (in terms of the decision strategy at the sensors) between a scenario with ideal communication links and a scenario with noisy communication links. Therefore, the derivation considered in Subsection 3.1.2 for sensor threshold selection holds in this case as well.

We remark that the proposed BSC model for a communication link is realistic for a sensor network where there are strong Line-Of-Sight (LOS) communication channels between the sensors and AP. In this case, each communication link can be modelled as an Additive White Gaussian Noise (AWGN) channel, and the cross-over probability can be given an explicit expression depending on the considered coding/modulation format. For instance, in the case of uncoded Binary Phase Shift Keying (BPSK), the cross-over probability can be written as follows (Proakis, 2001):

$$p = Q\left(\sqrt{2\gamma_b}\right) = \int_{\sqrt{2\gamma_b}}^{\infty}\frac{1}{\sqrt{2\pi}}e^{-\frac{y^2}{2}}\mathrm{d}y \tag{10}$$

where $Q(x) \triangleq 1 - \Phi(x)$ and γ_b is SNR at AP (at the output of a communication link). This illustrative mapping of the cross-over probability p into a realistic model for the communication links underlines that our conclusions are meaningful also for practical (wireless) sensor networks. Moreover, it would be possible to extend our framework in order to take directly into account link communication constraints, such as, for example, the available bandwidth (Xiao and Luo, 2005). In order to model a communication link with fading, we point out, however, that a BSC model might not be the most appropriate one. Other models, such as Binary Erasure Channel (BEC) (Cover and Thomas, 1991), might be more suitable.

3.3 Absence of quantisation

The previous analysis holds when each sensor makes a binary decision about the observed phenomenon, i.e. there is a two-level quantisation of the corresponding observable. Such a design choice could be motivated by the limited bandwidth of realistic communication links. At the other extreme, one can evaluate the network behaviour when no quantisation is considered at the sensors. In this case, the conditional PDF of the observed signal, rather than a single bit, is transmitted to AP. Obviously, this is not practical, but gives important indications about the improvement brought by the use of quantisation.

In the absence of quantisation, AP decision is based on the received observations vector $\mathbf{r} = \{r_1, r_2, \ldots, r_N\}$. Under the Maximum A posteriori Probability (MAP) detection criterion, the decision rule at AP is the following:

$$u_0 = \begin{cases} H_0 & \text{if} \quad p(\mathbf{r}|H_0)P(H_0) > p(\mathbf{r}|H_1)P(H_1) \\ H_1 & \text{if} \quad p(\mathbf{r}|H_0)P(H_0) < p(\mathbf{r}|H_1)P(H_1) \end{cases} \quad (11)$$

where $p(\mathbf{r}|H) = \prod_{i=1}^{N} p(r_i|H)$ since all the sensor observations are supposed independent. After a few manipulations, equation (11) can be rewritten as

$$\hat{H} = \begin{cases} H_0 & \text{if} \quad \ln \dfrac{P(H_0)}{P(H_1)} + \sum_{i=1}^{N} \ln \dfrac{p(r_i|H_0)}{p(r_i|H_0)} > 0 \\ H_1 & \text{if} \quad \ln \dfrac{P(H_0)}{P(H_1)} + \sum_{i=1}^{N} \ln \dfrac{p(r_i|H_0)}{p(r_i|H_0)} < 0. \end{cases} \quad (12)$$

Since the observable r_i has the form discussed in Section 2, the decision rule (12) can be expressed as

$$\hat{H} = \begin{cases} H_0 & \text{if} \quad \ln \dfrac{P(H_0)}{P(H_1)} + \sum_{i=1}^{N} \left(\dfrac{-r_i s_i}{\sigma_i^2} + \dfrac{s_i^2}{2\sigma_i^2} \right) > 0 \\ H_1 & \text{if} \quad \ln \dfrac{P(H_0)}{P(H_1)} + \sum_{i=1}^{N} \left(\dfrac{-r_i s_i}{\sigma_i^2} + \dfrac{s_i^2}{2\sigma_i^2} \right) < 0. \end{cases} \quad (13)$$

Based on equation (13), the two conditional probabilities in equation (2) become, respectively:

$$P(u_0 = H_1 | H = H_0) = P\left\{ \sum_{i=1}^{N} \frac{n_i s_i}{\sigma_i^2} > \sum_{i=1}^{N} \frac{s_i^2}{2\sigma_i^2} + \ln \frac{P(H_0)}{P(H_1)} \right\} \quad (14)$$

$$P(u_0 = H_0 | H = H_1) = P\left\{ \sum_{i=1}^{N} \frac{n_i s_i}{\sigma_i^2} < -\sum_{i=1}^{N} \frac{s_i^2}{2\sigma_i^2} + \ln \frac{P(H_0)}{P(H_1)} \right\}. \quad (15)$$

Since $\{n_i\}$ are independent Gaussian random variables with zero mean and variance equal to one, it follows that $\sum_{i=1}^{N} n_i s_i / \sigma_i^2 \sim N\left(0, \sum_{i=1}^{N} s_i^2 / \sigma_i^2\right)$ (Papoulis, 1991). Therefore, in a scenario with no quantisation at the sensors, the probability of decision error equation (2) can be finally written as follows:

$$P_e = \Phi\left(\frac{\ln \dfrac{P(H_0)}{P(H_1)} - \sum_{i=1}^{N} \dfrac{s_i^2}{2\sigma_i^2}}{\sqrt{\sum_{i=1}^{N} \dfrac{s_i^2}{2\sigma_i^2}}} \right) P(H_0)$$
$$+ Q\left(\frac{\ln \dfrac{P(H_0)}{P(H_1)} + \sum_{i=1}^{N} \dfrac{s_i^2}{2\sigma_i^2}}{\sqrt{\sum_{i=1}^{N} \dfrac{s_i^2}{2\sigma_i^2}}} \right) P(H_1). \quad (16)$$

4 Sensor SNR profiles

As observed in the previous section, the probability of decision error ultimately depends on the *sensor SNR profile* $\{\mathrm{SNR}_{\mathrm{sensor}}^{(i)}\}$. A generic example of sensor SNR profile is shown in Figure 1(a): the sensor SNRs are generally not monotonically ordered. However, since it is always possible to reorder the sensor SNRs from highest to lowest, as shown in Figure 1(b), without loss of generality, one can restrict his/her attention to a scenario where the sensor SNR profile is *non-increasing*.

Based on the observation in the previous paragraph, in order to characterise non-increasing sensor SNR profiles we consider four possible cases (SNRs are expressed in dB):

Linear profile : $\quad \mathrm{SNR}_i = \mathrm{SNR}_0 - c \cdot i$
Quadratic profile: $\quad \mathrm{SNR}_i = \mathrm{SNR}_0 - c \cdot i^2$
Cubic profile : $\quad \mathrm{SNR}_i = \mathrm{SNR}_0 - c \cdot i^3 \quad (17)$
Hyperbolic profile: $\mathrm{SNR}_i = \dfrac{\mathrm{SNR}_0}{1 + c \cdot i},$

where $i = 0, \ldots, N-1$; N is the number of sensors; SNR_0 is the highest sensor SNR; and c is a suitable constant which uniquely characterises the sensor SNR profile *slope*. For this reason, we denote c as *slope coefficient*. A large value of c corresponds to a scenario where the sensor SNRs decrease rapidly (i.e. the corresponding realistic non-ordered sensor

SNR profile is highly varying), whereas a small value of c corresponds to a scenario where the sensor SNRs are similar (i.e. the corresponding realistic non-ordered sensor SNR profile is almost constant). If $c = 0$, all profiles degenerate to a constant profile, i.e. $SNR_i = SNR_0, \forall i$. In Figure 1(b), illustrative graphical examples of the four profiles are shown. We remark that both convex (linear, quadratic and cubic) and concave (hyperbolic) profiles are being considered. As one can see, by suitably setting the values of SNR_0 and c, a large number of realistic sensor SNR profiles can be characterised. This underlines the applicability of our framework. In Section 7, we will propose a simple experiment to characterise a realistic sensor SNR profile.

Figure 1   Illustrative sensor SNR profile: (a) realistic and (b) reordered with non-increasing values of SNRs. In particular, in part (b) four possible interpolating profiles (linear, quadratic, cubic and hyperbolic) are shown (see online version for colours)
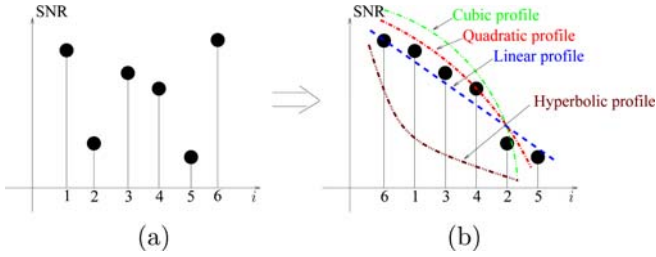
In equation (17), we have assumed that the maximum SNR and the slope coefficient c are the same for all profiles. However, in this case the winning profile is always the linear, since the sensor SNR at any position is higher than the corresponding one in any other profile. In order to obtain a 'fair' comparison between the various profiles, one can impose that all SNR profiles have the same average value, denoted as $\overline{SNR}$.

- By imposing that the slope coefficient c is the same for all profiles, after a few manipulations one obtains that the maximum SNRs in the various cases need to be set as follows:

$$SNR_{0,1} = \overline{SNR} + c\frac{N-1}{2}$$

$$SNR_{0,q} = \overline{SNR} + c\frac{(N-1)(2N-1)}{6}$$

$$SNR_{0,c} = \overline{SNR} + c\frac{N(N-1)^2}{4} \qquad (18)$$

$$SNR_{0,h} = \frac{N \cdot \overline{SNR}}{\sum_{i=0}^{N} \frac{1}{(1+c \cdot i)}}.$$

- Specularly, imposing that the maximum SNR is the same for all the sensors, the slope coefficient in the four considered cases need to be set in the following way:[6]

$$c_1 = (SNR_0 - \overline{SNR})\frac{2}{N-1}$$

$$c_q = (SNR_0 - \overline{SNR})\frac{6}{(N-1)(2N-1)}$$

$$c_c = (SNR_0 - \overline{SNR})\frac{4}{N(N-1)^2} \qquad (19)$$

$$c_h = \sum_{i=0}^{N-1}\frac{1}{1+c_h \cdot i} = \frac{N \cdot \overline{SNR}}{SNR_0}.$$

Finally, one should observe that in equation (19) it must hold that $SNR_0 - \overline{SNR} \geq 0$ and $\overline{SNR}/SNR_0 \leq 1$.

We point out that throughout this paper we make the implicit assumption that SNR profiles are perfectly known and available at AP. This is expedient for performance analysis. However, in a realistic scenario, the mechanisms to collect SNR values from the resource-constrained sensors may not be very accurate, and relying too much on it may not be helpful. Collecting the values accurately is a challenging problem, which needs further investigation. For example, SNR values could be collected during a *training phase*, when each sensor computes its local SNR and send it to AP. In Section 7, we propose a simple experimental validation of our theoretical assumptions.

5   Performance results

5.1   Ideal communication links

Let us first consider a sensor network with ideal communication links from the sensors to AP. In Figure 2, the probability of decision error is shown, as a function of the number of nodes N, in scenarios with *linear*, *quadratic*, *cubic* and *hyperbolic* SNR profiles. For comparison, the performance in a scenario with *constant* SNR profile is also shown. The profiles have the same value of SNR_0, set to 12 dB, and (for non-constant profiles) the same slope coefficient $c = 0.25$. The a priori probabilities of the phenomenon are such that $P(H_0) = 10P(H_1)$: this is meaningful for situations where a phenomenon is rare (e.g. the phenomenon under observation is an unusually high humidity level). Both analytical results (according to the framework developed in the previous sections) and the Monte Carlo simulation results are shown as lines and symbols, respectively.[7] Obviously, the best performance is guaranteed by the constant SNR profile, since all sensors have the highest SNR (i.e. $SNR_0 = 12$ dB). One can observe that for a small number of sensors ($N \leq 3$), the performance with the hyperbolic profile degrades immediately, whereas the performance with linear, quadratic and cubic profiles is similar to that with the constant profile. For increasing number of sensors, the probability of decision error with cubic and quadratic profiles tends to increase rapidly, whereas the probability of decision error with a linear profile tends to flatten. This degradation, for increasing number of sensors, is due to the fact that, for a *fixed* value of the maximum sensor SNR, the average sensor SNR tends to

decrease for all non-constant profiles. This decrease is more rapid for cubic and hyperbolic profiles.

Figure 2 Probability of decision error, as a function of the number of the sensors N, in a scenario with linear, quadratic, cubic, hyperbolic and constant SNR profiles, with $SNR_0 = 12$ dB in all cases. The value of the coefficient c (for non-constant profiles) is $c = 0.25$ and $P(H_0) = 10P(H_1)$. The lines correspond to analytical results, whereas the symbols are associated with simulation results (see online version for colours)
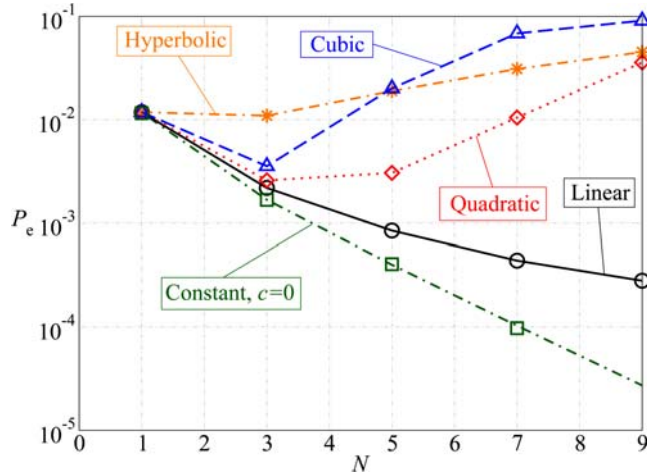
On the basis of the results shown in Figure 2, the following question is meaningful: for a given value of SNR_0, what are the conditions under which the use of a limited number of sensors (lower, for instance, than N) is the winning strategy? In order to answer this question, in Figure 3 the probability of decision error is shown, as a function of the coefficient c, in a scenario with linear SNR profile and $P(H_0) = 10P(H_1)$. The lines correspond to analytical results, whereas the symbols are associated with the Monte Carlo simulation results. Two possible values for the highest sensor SNR, i.e. SNR_0, are considered: 12 and 16 dB, respectively. For each value of the sensor SNR, various numbers of sensors are considered. Obviously, the curves corresponding to scenarios with only $N = 1$ sensor are constant with respect to c. The impacts of the parameters c and SNR_0 can be characterised as follows.

- For *small* values of c, i.e. in a scenario with almost constant SNR profile, the best performance is obtained using *all sensors*, regardless of the value of SNR_0.

  For *large* values of c (i.e. irregular sensor SNR profile before monotonic reordering), the best performance is obtained using only the sensors with *the highest SNR*. Note that the best asymptotic performance ($c \to \infty$) is obtained using only *the* sensor with highest SNR (SNR_0); however, the probability of decision error might be intolerably high.

- For low values of SNR_0, the impact of c is 'mild', whereas for high values of SNR_0 the impact of c is relatively stronger. This behaviour can be interpreted as follows. If *at least* one sensor is highly accurate, i.e. SNR_0 is high, then in order to optimise the network

performance the right subset of sensors should be carefully chosen. In other words, the higher is the sensitivity of at least one sensor in observing the phenomenon, the more accurate the selection of a suitable subset of sensors has to be carried out.

As one can observe from Figure 3, for a given value of c, the best performance is obtained selecting a specific number of sensors – those with highest SNRs, starting from the one with SNR_0. In order to characterise this behaviour in more detail, in Figure 4 the optimal value of the number of sensors to be selected is shown, as a function of c, for various values of SNR_0. The results in Figure 4 show that (i) the optimal number of sensors is a decreasing function of c, and (ii) the lower is SNR_0, the faster the optimal number of sensors decreases for increasing values of c. A careful reader might wonder, at this point, why the optimal number of sensors does not reduce by one in correspondence with each vertical (decreasing) step. This behaviour is due to the fact that the decision threshold τ_i at ith sensor is computed according to equation (6), which represents a *locally optimal* threshold selection strategy. Therefore, one can conclude that such a threshold selection strategy is not *globally optimal* (from the entire distributed decision process), as already observed in Willett et al. (1992). The individuation of globally optimal decision thresholds at the sensors in a scenario with non-constant sensor SNR profile is currently under investigation. However, *given that* the local thresholds are selected according to (6), the results presented in this paper are *correct*.

Figure 3 Probability of decision error, as a function of the coefficient c, with SNR_0 equal to 12 and 16 dB, respectively. Various values of the number of sensors N are considered, in a scenario with *linear* sensor SNR profile and $P(H_0) = 10P(H_1)$. The lines correspond to analytical results, whereas the symbols are associated with simulation results (see online version for colours)
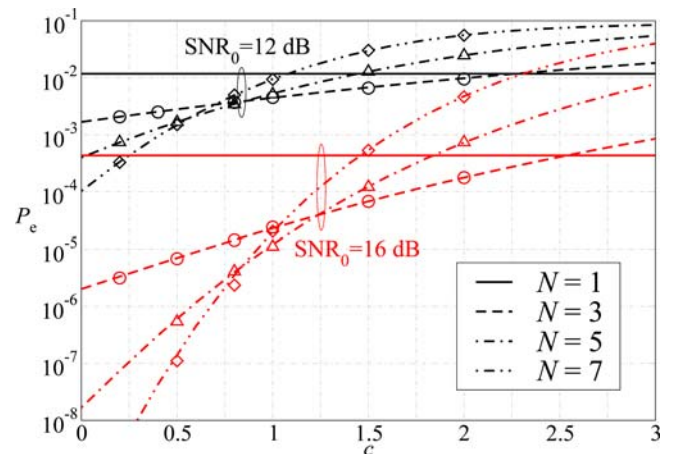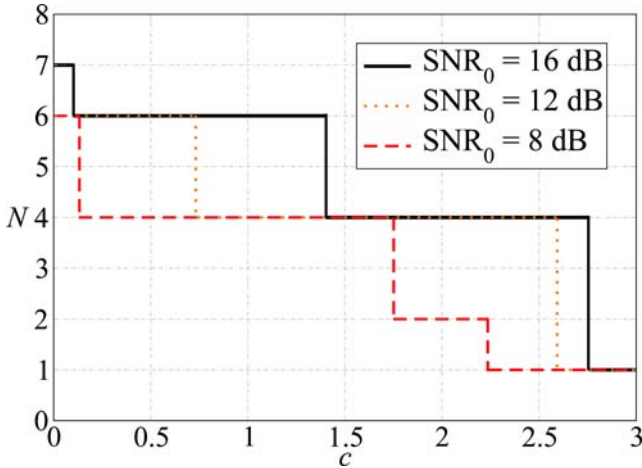

In Figure 5, the probability of decision error is shown, as a function of the number of sensors N, for the same scenario considered in Figure 2, but imposing a common *average* sensor SNR value $\overline{(SNR)}$, rather than a common maximum sensor SNR value (SNR_0), as shown in Figure 2. Unlike

Figure 2, one can observe that in Figure 5 the probability of decision error is a decreasing function of N in all considered cases. In other words, increasing the number of sensors makes the probability of decision error lower and lower. In this case, it turns out that the winning SNR profile is the cubic. Comparing Figure 2 with Figure 5, one can conclude that:

- for a common value of SNR_0, the *higher* is the *irregularity* of the sensor SNR profile, the *worse* is the network performance – the best non-increasing profile is the linear;

- for a common value of $\overline{SNR}$, the *higher* is the *irregularity* of the sensor SNR profile, the *better* is the network performance.

Figure 4   'Optimal' number of sensors (for minimising the probability of decision error) as a function of the coefficient c, in a scenario with *linear* sensor SNR profile and $P(H_0) = 10P(H_1)$. Three values for SNR_0 are considered (two of them are the same as in Figure 3) (see online version for colours)

In order to evaluate the impact of the slope coefficient c on the network performance, we impose both a common *maximum* sensor SNR (i.e. a common value of SNR_0) and a common *average* sensor SNR (i.e. a common value of $\overline{SNR}$). The corresponding values of the coefficient c for all considered profiles are chosen according to equation (19). In Figure 6, the probability of decision error is shown as a function of the number of sensors N. The average sensor SNR is set as in Figure 5 and two possible values for the maximum sensor SNR are considered: (i) $SNR_0 = 14$ dB (solid lines) and (ii) $SNR_0 = 20$ dB (dashed lines). One can observe that in the case with $SNR_0 = 14$ dB all the curves overlap, i.e. the optimised values of c (according to equation (19)) lead to the same performance for all the considered profiles (i.e. linear, quadratic, cubic and hyperbolic). In the case with $SNR_0 = 20$ dB, instead, the performance differs from profile to profile and the winning profile is the cubic, as in a scenario with common values of average sensor SNR and slope coefficient (see Figure 5). This can be explained as follows. For a given average sensor SNR, a cubic profile is such that there is a relatively larger number of

sensors with high SNR and, consequently, a larger number of sensors with low SNR. Therefore, this suggests that the network performance tends to be optimised if, for a given average sensor SNR, the variance of the sensor SNRs is larger.

Figure 5   Probability of decision error, as a function of the number of sensors N, for the same scenario of Figure 2 and a common *average* value $\overline{SNR} = 12$ dB. The lines correspond to analytical results, whereas the symbols are associated with simulation results (see online version for colours)
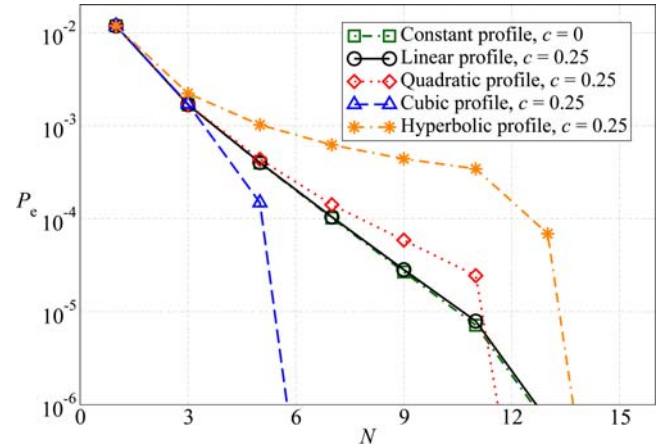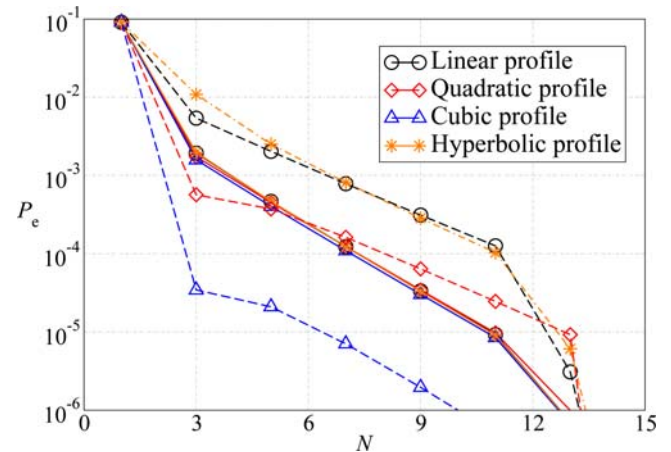

Figure 6   Probability of decision error, as a function of the number of sensors N, with $\overline{SNR} = 12$ dB (as in Figure 5). Two possible common values for SNR_0 are considered: (i) $SNR_0 = 14$ dB (solid lines) and (ii) $SNR_0 = 20$ dB (dashed lines) (see online version for colours)


From the results shown in Figure 6, one could ask himself/herself what is the relative role played by the two common parameters in equation (19), i.e. SNR_0 and $\overline{SNR}$. In order to answer this question, in Figure 7 the sensor SNR profile is shown in the two scenarios considered in Figure 6: (a) $\overline{SNR} = 12$ dB and $SNR_0 = 14$ dB and (b) $\overline{SNR} = 12$ dB and $SNR_0 = 20$ dB.[8] From the results in Figure 6 and Figure 7, the following comments can be made.

- The parameter $\overline{SNR}$ determines the profile *shape*, i.e. how the sensor SNR decays as a function of the number

of nodes. However, the shape remains approximately the same for the considered values of SNR_0, as one can see comparing Figure 7(a) with Figure 7(b). The only difference consists of a 'compression' of the profiles along the vertical axis.

- The parameter SNR_0 or, more precisely, the distance between SNR_0 and $\overline{\text{SNR}}$, determines (as shown in Figure 6) the network performance and the winning profiles, i.e. the profile which guarantees the lowest probability of decision error.

Figure 7 Sensor SNR profiles for $N = 11$ and $\overline{\text{SNR}} = 12$ dB. Two values of SNR_0 are considered: (a) $\text{SNR}_0 = 14$ dB and (b) $\text{SNR}_0 = 20$ dB. All the possible interpolating profiles of interest (linear, quadratic, cubic and hyperbolic) are shown (see online version for colours)
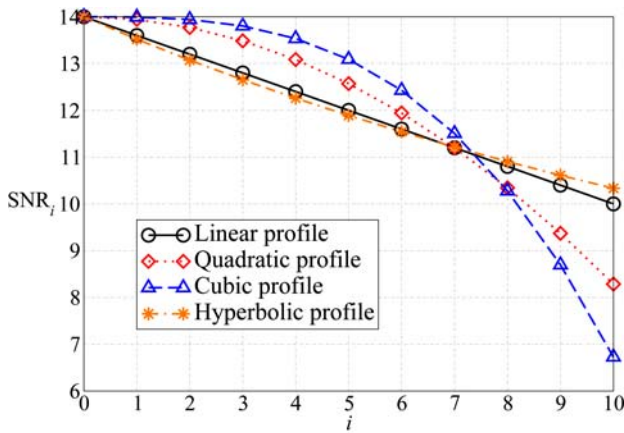

(a)
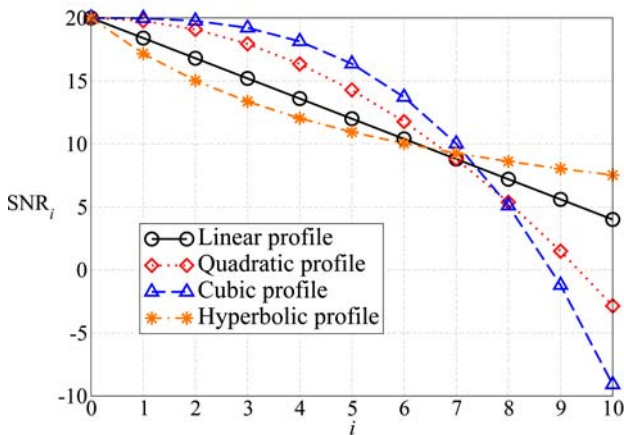
(b)

In Figure 8, the probability of decision error is shown, as a function of the maximum sensor SNR (i.e. SNR_0), in a scenario with $\overline{\text{SNR}} = 12$ dB and $N = 11$ sensors. All the proposed profiles for the sensor SNRs (i.e. linear, quadratic, cubic and hyperbolic) are considered. One can observe that the cubic profile is the winning profile for a sufficiently high maximum sensor SNR (as previously shown in Figure 6), whereas the other profiles have a worse performance and the corresponding probability of decision error seems to reach a floor. The fact that the cubic profile is the winning

can be motivated on the basis of the results in Figure 7. In fact, we have observed that for a reduced subset of sensors the cubic profile has sensor SNR values (relatively) higher than the corresponding ones in the other profiles considered in this paper. Moreover, in Figure 2 it is shown that a proper choice of a sensor subset can minimise the probability of decision error, since the performance is dominated by the sensor with the highest SNR.

Figure 8 Probability of decision error, as a function of the maximum sensor SNR, in a scenario with $\overline{\text{SNR}} = 12$ dB and $N = 11$ sensors. All the proposed sensor SNR profiles (linear, quadratic, cubic and hyperbolic) are considered (see online version for colours)
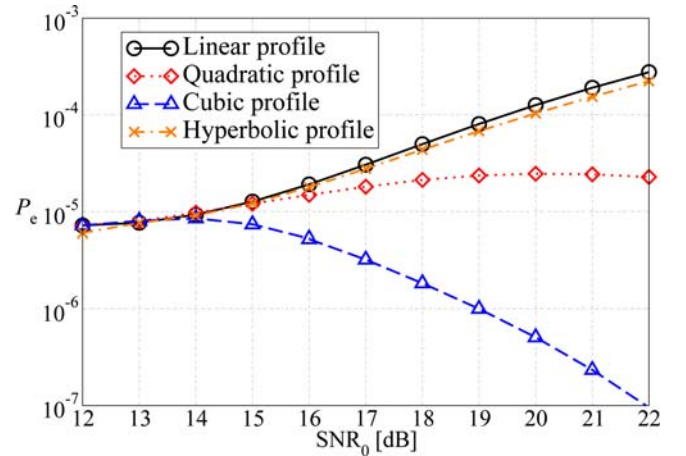
5.2 Noisy communication links

While in the previous subsection, we have considered a scenario with *ideal* communication links, we now extend the previous analysis in order to evaluate the impact of the sensor SNR profile in the presence of noisy communication links. More precisely, in a simple network scenario with $N = 3$ sensors, we compare directly the performance with linear, quadratic and cubic sensor SNR profiles. We do not consider the hyperbolic profile, since we have shown in Subsection 5.1 that the overall performance with this profile is worse than that with the other profiles – in fact, in the presence of a hyperbolic profile the average sensor SNR has to be very high in order to obtain an acceptable performance level. We evaluate the probability of decision error in a scenario with *all noisy* communication links (considering two values for the cross-over probability p, equal to 10^{-3} and 10^{-1}, respectively) and, for comparison, in a scenario with all ideal links. In Figure 9, the probability of decision error is shown, as a function of the slope coefficient c, in various scenarios with $\text{SNR}_0 = 16$ dB and $P(H_0) = 10P(H_1)$. In Figure 10, the same sensor network scenario is considered, but the *average* sensor SNR is kept constant to $\overline{\text{SNR}} = 16$ dB – for each value of c, the corresponding value of SNR_0 is determined according to equation (18). On the basis of the results shown in Figures 9 and 10, it is possible to characterise, performance-wise, the interaction between the sensor SNR profile and the communication noise as follows.

- In a scenario with *common* value of SNR_0, the impact of the sensor SNR profile is very similar in scenarios with ideal communication links and with noisy communication links. For the same value of *c*, the probability of decision error increases if the profile changes from linear to cubic. Obviously, for *c* = 0 the performance with the three profiles coincides. Moreover, asymptotically (for large values of *c*) the probability of decision error is the same regardless of the profile. Therefore, it is possible to identify a critical value of *c* beyond which the impact of the sensor SNR profile is the highest. The impact of the noise is strong for small values of *c*, whereas it becomes negligible for large values of *c*. In fact, for any given profile, the curves associated with ideal links and those associated with noisy links tend to coincide for increasing values of *c*. In other words, the less regular is the sensor SNR profile (i.e. the larger is *c*), the milder is the impact of the noise in the communication links. On the other hand, if the sensor SNR is very similar across the sensors, then the noise in the communication links has a severe impact of the network performance. This latter scenario is analysed in detail in Ferrari and Pagliari (2006).

- In a scenario with a common value of $\overline{SNR}$, rather than a common maximum sensor SNR, the $P_e - c$ curves do not tend to coincide for large values of the slope coefficient *c*. In other words, the impact of value of *c* in a scenario with common $\overline{SNR}$ is stronger than in a scenario with common SNR_0. On the other hand, for small values of the slope coefficient *c*, the performance in a scenario with common $\overline{SNR}$ is similar to that in a scenario with common SNR_0. From the results in Figure 10, one can also make another observation. In the presence of ideal communication links, for increasing values of *c* the best performance is obtained by quadratic and cubic profiles (this was expected from the results in Figure 5). In contrast, in the presence of noisy communication links, for increasing values of *c* the best performance is given by a linear sensor SNR profile.

5.3 *Absence of quantisation*

In Figure 11, the probability of decision error is shown, as a function of *N*, when no decision is made at the sensors, i.e. the sensors transmit to AP their observation likelihoods. The a priori probabilities of the phenomenon are such that $P(H_0) = 10P(H_1)$. The sensor SNR profiles are the same of those considered in Figure 2, i.e. linear, quadratic, cubic and hyperbolic, and the slope coefficient is fixed to *c* = 0.25. For comparison, the results for a constant profile (i.e. *c* = 0) are also shown. As in Figure 2, one can observe that the higher is the irregularity of SNR profile, the worse is the performance. In this case as well, there exists an optimum value of *N* which minimises the probability of decision error, but it is higher than the equivalent one in a scenario

with local binary decisions (i.e. two-level quantisation at the sensors).

Figure 9 Probability of decision error, as a function of the coefficient *c*, in a scenario with *N* = 3 sensors and $P(H_0) = 10P(H_1)$. The common value of the maximum sensor SNR is SNR_0 =16 dB. Three possible scenarios are considered: (i) all ideal links (*p* = 0) and all noisy links with (ii) $p = 10^{-3}$ and (iii) $p = 10^{-1}$, respectively. For comparison, the performance with *N* = 1 sensor is also shown (horizontal solid line) (see online version for colours)
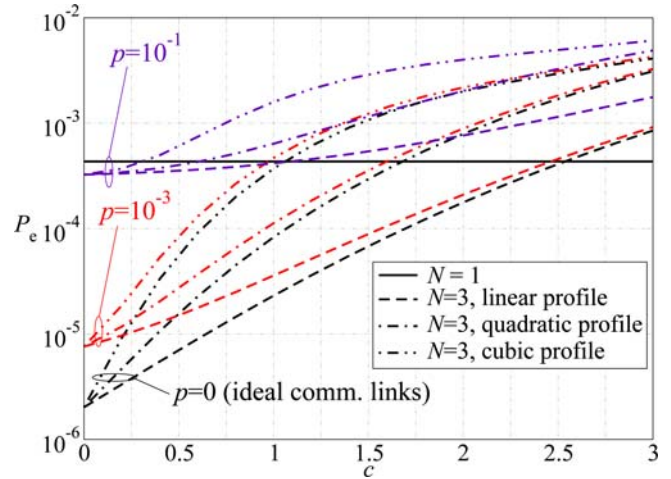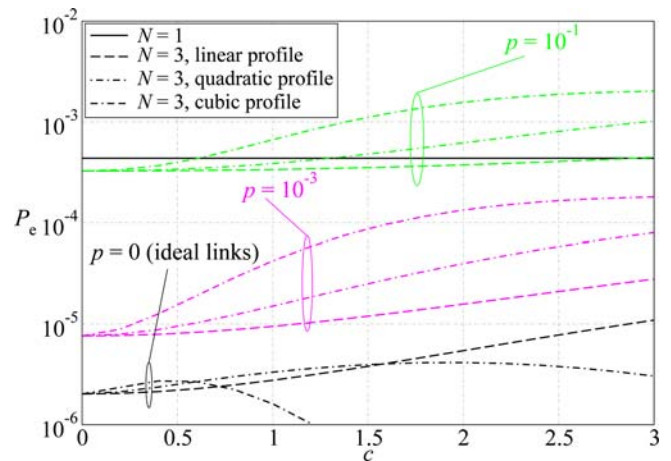
Figure 10 Probability of decision error, as a function of the coefficient *c*, for the same scenario of Figure 9 and a common *average* value of the sensor SNR equal to $\overline{SNR}$ = 16 dB (see online version for colours)

Comparing Figure 11 with Figure 2, one can observe that, for a given value of *N*, equivalent curves are different: obviously, for a given sensor SNR, the probability of decision error in the absence of quantisation is lower than that in the presence of quantisation. In fact, transmission of PDF from a sensor to AP leads to no local loss of information. The obtained performance, therefore, can be interpreted as a *lower bound* for the performance of any realistic decentralised detection scheme. In practice, this lower bound can be approached using a sufficiently large number of quantisation levels at the sensors. Finally, one can observe that, also in the case with no

quantisation at the sensors, simulation and analytical results are in excellent agreement.

Figure 11 Probability of decision error, as a function of the number of sensors N, in the absence of quantisation and in the same scenario considered in Figure 2. Various sensor SNR profiles are considered: linear, quadratic, cubic and hyperbolic (with $c = 0.25$), and constant (i.e. $c = 0$). Lines correspond to analytical results, whereas symbols are associated with simulation results (see online version for colours)
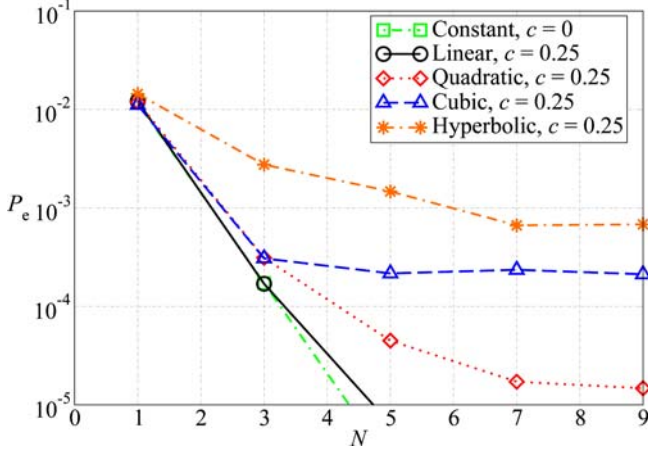
6 Asymptotic analysis

In the previous sections, we have proposed a simple, yet effective, framework for performance analysis of a sensor network with non-constant SNR profile. In order to investigate the asymptotic (for large sensor SNR) network performance, we analyse the limiting behaviour of the conditional probability $P(u_0 = H_1|H_0)$ in equation (8) when SNR_0 becomes increasingly large – the same approach can be considered for the evaluation of $P(u_0 = H_0|H_1)$.

Taking into account the results in Section 2, one obtains

$$\lim_{SNR_0 \to \infty} P(u_l^{rec} = H_i|H_j) = p, \qquad i \neq j \qquad (20)$$

$$\lim_{SNR_0 \to \infty} P(u_l^{rec} = H_i|H_j) = 1 - p, \quad i = j \qquad (21)$$

where $i, j = 0, 1$. Using equations (20) and (21) in equation (9) (and in similar terms appearing in the expression for the probability of decision error), it follows:

$$P_e^{asym} \triangleq \lim_{SNR_0 \to \infty} P_e = P(H_0) \sum_{i=k}^{N} \binom{N}{i} p^i (1-p)^{N-i}$$
$$+ P(H_1) \sum_{i=0}^{k-1} \binom{N}{i} (1-p)^i p^{N-i} \qquad (22)$$

which is the same relation given in Ferrari and Pagliari (2006) for a constant SNR profile. This result implies that, asymptotically, the network performance is dominated by the sensor with the highest SNR, i.e. SNR_0. In other words, for a sufficiently high value of SNR_0, the sensor network

behaves *as if* the profile were constant and equal to SNR_0. All the analysis developed in Ferrari and Pagliari (2006) for a scenario with constant sensor SNRs can then be applied in this asymptotic $(SNR_0 \to \infty)$ regime.

Figure 12 Asymptotic $(SNR_0 \to \infty)$ probability of decision error, as a function of the cross-over probability p of the noisy communication links. Various values of the number of sensors N are considered. Both exact results (solid lines) and approximate results with the DeMoivre–Laplace approximation (dashed lines) are shown (see online version for colours)
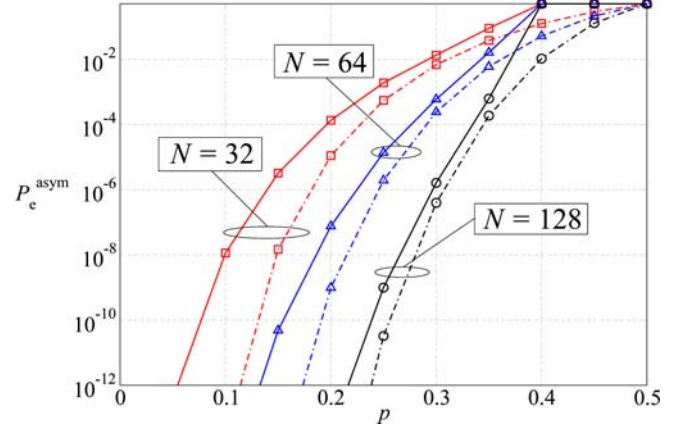
At this point, it is interesting to evaluate what happens when not only the sensor SNRs are large but also the number of sensors N becomes large. Applying the De Moivre–Laplace theorem (Papoulis, 1991), we can approximate the binomial distributions within the two terms in equation (22) as Gaussian distributions with means, respectively, Np and $N(1 - p)$, and with the same variance $Np(1-p)$. After a few manipulations, one obtains:

$$P(u_0 = H_1|H_0) \simeq Q(\alpha(p)\sqrt{N})$$

$$P(u_0 = H_0|H_1) \simeq Q(\beta(p)\sqrt{N})$$

where $\alpha(p) \triangleq (0.5 - p)/\sqrt{p(1-p)}$, and $\beta(p) \triangleq -\alpha(p)$. Using the fact that $Q(-x) = 1 - Q(x)$, the limiting probability of decision error equation (22) can be finally approximated as follows:

$$P_e^{asym} \simeq Q(\alpha(p)\sqrt{N}), \quad N \gg 1. \qquad (23)$$

Note that the final approximate expression (23) *no longer* depends on the a priori probabilities of the phenomenon (i.e. $P(H_0)$ and $P(H_1)$). In Figure 12, the performance obtained using equation (23) is shown and compared with the exact probability of decision error. As expected, the probability of decision error increases when the noise level (i.e. the cross-over probability p) increases, due to the fact that transmissions are less reliable. Besides, for low values of p the performance improves because the communication noise level is not high and, consequently, the probability of decision error decreases to zero. The approximate expression (23)

becomes more and more accurate when the number of sensors N increases. This is due to the fact that the De Moivre–Laplace theorem is verified with high accuracy when $Np \gg 1$, i.e. when the number of sensors is sufficiently large (for a given value of p). Note that we have not specified the sensor SNR profile, since all profiles lead to the same performance in an asymptotic ($SNR_0 \to \infty$) regime. In fact, when SNR_0 is sufficiently large, all profiles described in equation (17) behave as a constant profile (as discussed at the beginning of this section).

7   Experimental validation

In this section, we show experimental results relative to SNRs measured at the sensors, in order to validate the theoretical models proposed in this paper. In particular, we evaluate the *Received Signal Strength Indication* (RSSI) in order to obtain *sensor SNR-like* profiles. Equivalently to the RSSI, one could also use the *Path Loss* indicator. In fact, the following equation (in logarithmic scale) holds:

$$P_t = \text{RSSI} + \text{Path Loss}$$

where P_t is the transmit power (dimension: [dBm]) and Path Loss is the power reduction incurred by propagation (dimension: [dB]). Since in our experiments we set $P_t = 0$ dBm, one easily obtains:
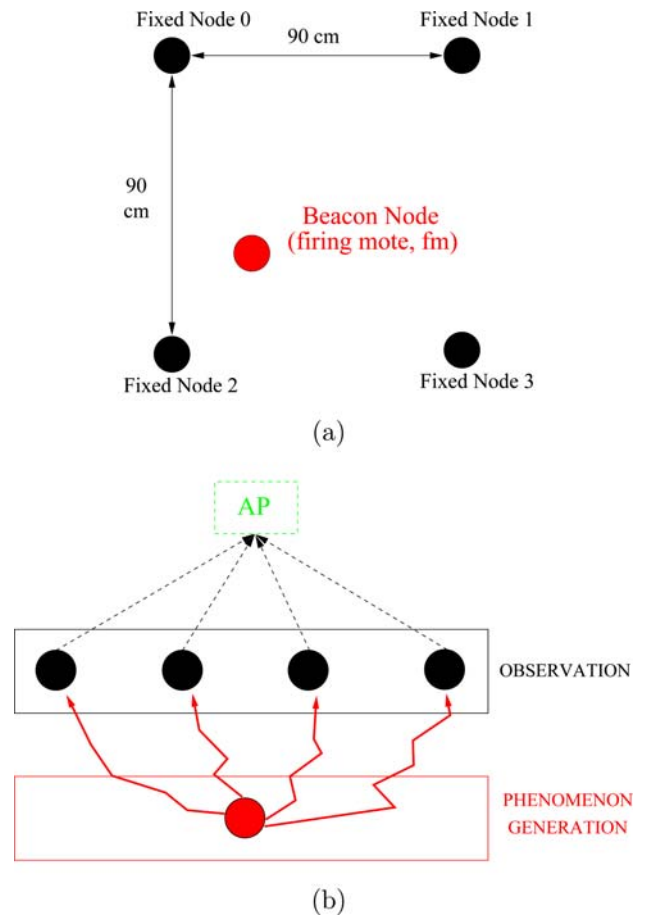
$$\text{RSSI} = -\text{Path Loss}.$$

The main idea of our experiments is as follows. A mobile mote sends periodically a message, called *beacon*, whereas N remote nodes, at fixed positions with respect to the mobile mote, receive the beacon and store the received power. Finally, a vector of N power levels is obtained, and an SNR-like profile can be derived. The experimental set-up[9] is schematically shown in Figure 13, from (a) practical and (b) logical viewpoints, respectively. We deploy four MicaZ nodes at the vertices of a square area of 90×90 cm^2, and the remaining mobile (beacon) mote acts as the event 'generator' and is denoted as *Firing Mote* (fm). As shown in Figure 13, four nodes are placed at the vertices of the network surface. The fm moves inside the network, sending messages to the fixed nodes. Note that in the considered experimental set-up, the observed phenomenon corresponds to the message sent by the mobile node. In order to replicate the theoretical analysis, after receiving the message from the fm, the four fixed nodes should take a decision (e.g. based on the received power), and send their decisions to an AP. Since our goal, in this section, is to characterise the sensor SNR profile, we do not consider the communication phase from the sensors to AP.

Two experiments have been run:

a   the fm, which sends the beacon, is very close to one of the remote (fixed) nodes;

b   the fm is in the middle between the network centre and one of the four vertices of the square network surface, i.e. a fixed node.

In Figure 14, the Path Loss is shown, as a function of the remote node IDs (indicated in Figure 13(a)), in two different scenarios: (a) fm is very close to one of the fixed nodes and (b) fm is in the middle between the network centre and one of the fixed nodes. As one can see from Figure 14(a), the lowest Path Loss is obtained, as expected, in correspondence to the nearest remote node. In this case, the profile described is a *heavyside-like* function, since only the fixed node closest to fm senses a high RSSI (or, equivalently, a low Path Loss), while the others do the opposite. In Figure 14(b), fm is in a more central region and, therefore, the measured power profile is, as expected, smoother than that observed in Figure 14(a).

Figure 13   Experimental set-up: (a) practical scheme with five motes (one 'firing/beacon node' and four fixed nodes), deployed over a square network surface with area equal to 90×90 cm^2 and (b) its corresponding logical scheme. The considered platforms are constituted by MicaZ motes using a communication protocol compliant with the IEEE 802.15.4 standard (see online version for colours)

Rearranging the values in Figure 14(b) in an increasing order, one can obtain a decreasing profile, as described in the previous sections, of Path Loss or RSSI measures. In Figure 15, the *Path Loss* profile is shown, as a function of the mote ID, for the four different cases (relative to the position of the mobile mote) considered in Figure 14(b). As one can observe, on the average, the profile is approximately linear.

Figure 14 Path Loss profiles in the presence of four MicaZ motes sensing fm. Fm is placed either (a) very close to one of the vertices or (b) between the centre of the area and one of the vertices (see online version for colours)
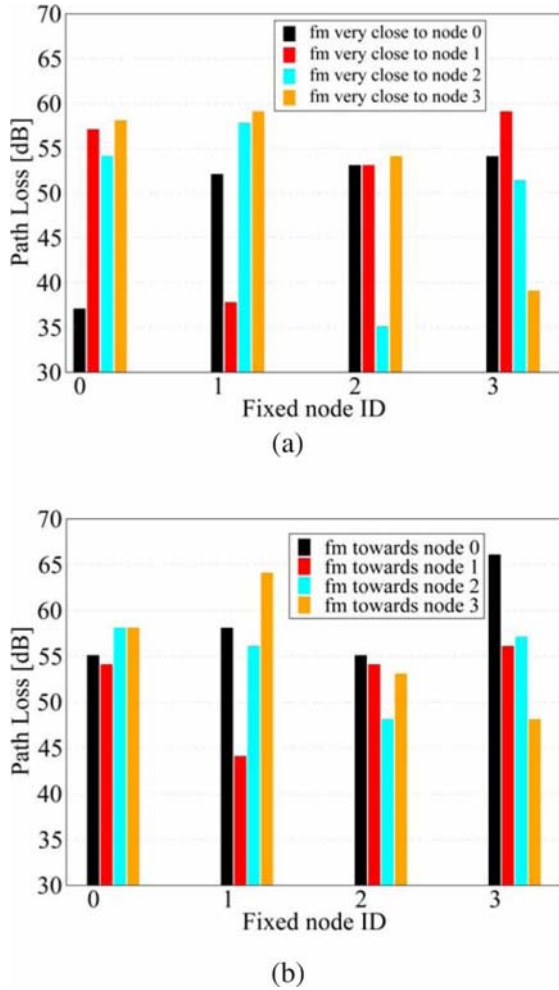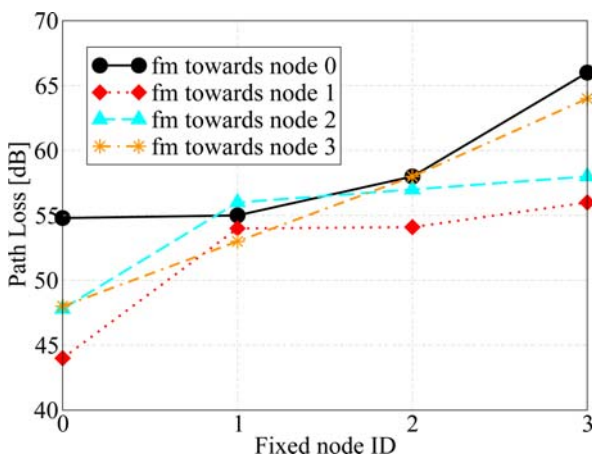

(a)

(b)

Figure 15 Reordered Path Loss profiles in the scenarios considered in Figure 14(b) (see online version for colours)

aware of the particular observation quality at each sensor. The sensors, however, optimise their decision thresholds according to their corresponding SNRs. In order to model this scenario, we have considered four possible sensor SNR profiles (linear, quadratic, cubic and hyperbolic) and we have characterised them by using a *slope coefficient* and the *maximum sensor SNR*. For increasing steepness of the (ordered) sensor SNR profile,i.e. for an increasingly irregular realistic sensor SNR profile, the best performance is obtained by selecting a lower and lower number of sensors (those with highest SNRs). In a scenario with common *average* sensor SNR, the profile which guarantees the best performance is the *cubic*. This is due to the fact that it corresponds to the profile with the largest (in relative terms) number of sensors with SNR higher than the average value. Therefore, a general conclusion is that, for a given *average sensor SNR*, the best performance is obtained when the variance of the sensor SNR is large, i.e. the sensor SNR profile is irregular. The presence of noisy communication links has also been considered. In this case, we have shown that the more irregular is the sensor SNR profile, the milder is the impact of the noise level in the communication links. In an *asymptotic* regime $(\mathrm{SNR}_0 \to \infty)$, when the sensor SNRs are sufficiently high and the number of sensors is sufficiently large, the performance no longer depends on the phenomenon a priori probabilities and the sensor SNR profile. Finally, we have considered a simple experimental approach to determine realistic sensor SNR profiles.

References

Alhakeem, S. and Varshney, P.K. (1995) 'A unified approach to the design of decentralized detection systems', *IEEE Transactions on Aerospace and Electronic Systems*, Vol. 31, No. 1, pp.9–20.

Blum, R.S., Kassam, S.A. and Poor, H.V. (1997) 'Distributed detection with multiple sensors − part II: advanced topics', *Proceedings of the IEEE*, Vol. 85, No. 1, pp.64–79.

Chen, B., Jiang, R., Kasetkasem, T. and Varshney, P.K. (2004) 'Channel aware decision fusion in wireless sensor networks', *IEEE Transactions on Signal Processing*, Vol. 52, No. 12, pp.3454–3458.

Chen, B. and Willett, P.K. (2005) 'On the optimality of the likelihood-ratio test for local sensor decision rules in t he presence of nonideal channels', *IEEE Transactions on Information Theory*, Vol. 51, No. 2, pp.693–699.

Chong, C-Y. and Kumar, S.P. (2003) 'Sensor networks: evolution, opportunities, and challenges', *Proceedings of IEEE*, Vol. 91, No. 8, pp.1247–1256.

Cover, T.M. and Thomas, J.A. (1991) *Elements of Information Theory*, Wiley, New York, NY.

Ferrari, G. and Pagliari, R. (2006) 'Decentralized binary detection with noisy communication links', *IEEE Transactions on Aerospace and Electronic Systems*, Vol. 42, No. 4, pp.1554–1563.

Gini, F., Lombardini, F. and Verrazzani, L. (1998) 'Decentralised detection strategies under communication constraints', *IEE Proceedings-Radar, Sonar and Navigation*, Vol. 145, No. 4, pp.199–208.

Hoballah, I.Y. and Varshney, P.K. (1989) 'An information theoretic approach to the distributed detection problem',

8 Concluding remarks

In this paper, we have analysed the performance of decentralised detection schemes in sensor networks where the observation SNRs differ from sensor to sensor, and AP is not

IEEE Transactions on Information Theory, Vol. 35, No. 5, pp.988–994.

Jiang, R. and Chen, B. (2005) 'Fusion of censored decisions in wireless sensor networks', *IEEE Transactions on Wireless Communications*, Vol. 4, No. 6, pp.2668–2673.

Papoulis, A. (1991) *Probability, Random Variables and Stochastic Processes*, McGraw-Hill, New York, NY.

Proakis, J.G. (2001) *Digital Communications*, 4th ed., McGraw-Hill, New York, NY.

Reibman, A. and Nolte, L. (1981) 'Detection with distributed sensors', *IEEE Transactions on Aerospace and Electronic Systems*, Vol. 17, No. 4, pp.501–510.

Reibman, A.R. and Nolte, L.W. (1988) 'On determining the design of fusion detection networks', In *Proceedings of the 27th Conference on Decision and Control*, Austin, TX, USA, pp. 2474–2478.

Tsitsiklis, J. (1988) 'Decentralized detection by a large number of sensor', *Mathematics of Control, Signals and Systems*, Vol. 1, No. 2, pp.167–182.

Viswanathan, R. and Varshney, P.K. (1997) 'Distributed detection with multiple sensors – part I: fundamentals', *Proceedings of IEEE*, Vol. 85, No. 1, pp.54–63.

Willett, P., Tober, B. and Swaszek, P. (1992) 'Fully-connected non-hierarchical decentralized detection networks', *Proceedings of IEEE Conference on Control Applications*, Dayton, OH, pp.404–409.

Xiao, J-J. and Luo, Z-Q. (2005) 'Universal decentralized detection in a bandwidth-constrained sensor network', *IEEE Transactions on Signal Processing*, Vol. 53, No. 8, pp.2617–2624.

Notes

1   For ease of notational conciseness, we do not explicitly indicate the epoch of the observations. However, we are assuming that all sensors simultaneously observe the common phenomenon.

2   In the presence of *ideal* communication links, $u_i^{\text{rec}} = u_i$. However, as it will be shown in the following, in the presence of *noisy* communication links it might happen that $u_i^{\text{rec}} \neq u_i$.

3   The events $\{H = H_0\}$ and $\{H = H_1\}$ will simply be denoted as H_0 and H_1, respectively.

4   Note that $\Omega_i(j)$ depends also on N. However, for the sake of notational simplicity, this dependence is not explicitly indicated. The context should eliminate any ambiguity.

5   We are implicitly assuming that each sensor estimates its own observation SNR.

6   The value of c_{h} in the last line of equation (19) cannot be given a closed-form expression, but can be numerically evaluated.

7   We point out that the analytical results are *exact*. This justifies the excellent agreement between analysis and simulations.

8   Note that the scale of the vertical axis of Figure 7(a) is different from that of Figure 7(b).

9   Since our experiments are developed in a laboratory environment, there is furniture all around the square area where the sensors are deployed. However, we can consider the reflected signals negligible.